Laser and Particle Beams (2010), *28*, 479–489.

doi:10.1017/S0263034610000479

Spatial evolution of a *q*-Gaussian laser beam in relativistic plasma

A. SHARMA AND I. KOURAKIS

Centre for Plasma Physics, School of Mathematics & Physics, Queen's University Belfast, Belfast, United Kingdom

(RECEIVED 16 April 2010; ACCEPTED 17 June 2010)

Abstract

In a recent experimental study, the beam intensity profile of the Vulcan petawatt laser beam was measured; it was found that only 20% of the energy was contained within the full width at half maximum of 6.9 μm and 50% within 16 μm, suggesting a long-tailed non-Gaussian transverse beam profile. A *q*-Gaussian distribution function was suggested therein to reproduce this behavior. The spatial beam profile dynamics of a *q*-Gaussian laser beam propagating in relativistic plasma is investigated in this article. A non-paraxial theory is employed, taking into account nonlinearity *via* the relativistic decrease of the plasma frequency. We have studied analytically and numerically the dynamics of a relativistically guided beam and its dependence on the *q*-parameter. Numerical simulation results are shown to trace the dependence of the focusing length on the *q*-Gaussian profile.

Keywords: Beam Dynamics; q-Gaussian; Relativistic Plasma

1. INTRODUCTION

The propagation of ultra-high intensity laser beams in plasmas has recently received significant attention, mainly due to their potential applications in the development of X-ray lasers (Faenov *et al.*, 2007; Svanberg & Wahlstrom, 1995), plasma-based accelerators (Joshi *et al.*, 2002; Tajima & Dawson, 1979; Nakajima *et al.*, 1995; Modena *et al.*, 2002; Gordon *et al.*, 1998; Malka *et al.*, 2002; Geddes *et al.*, 2004; Faure *et al.*, 2004; Mangles *et al.*, 2004; Lifschitz *et al.*, 2006; Singh *et al.*, 2010), and fast-ignition schemes for inertial confinement thermonuclear fusion (Deutsch *et al.*, 2008; Hora, 2007; Kline *et al.*, 2009; Tabak *et al.*, 1994; Romagnani *et al.*, 2008; Roth *et al.*, 2001; Seifter *et al.*, 2009). In all of these applications, it is necessary for a high intensity laser beam to propagate in a controllable manner over a long distance with high directionality. If the laser peak power is high enough, a laser beam can overcome the natural limit of refraction, and undergo a focusing effect in the plasma due to non-linear self-interaction (Askaryan, 1962; Litvak, 1969; Max *et al.*, 1974; Borisov *et al.*, 1992; Monot *et al.*, 1995). The balance between self-focusing and diffraction can provide a condition for long-distance propagation of beams with peak intensity higher than otherwise achievable in vacuum. Beam self-focusing is strongly affected by the transverse distribution of beam irradiance (Sodha & Faisal, 2008; Sodha *et al.*, 1976; Sodha *et al.*, 1974). In a recent series of investigations, Sodha *et al.* (2009*a*, 2009*b*) have presented a modified paraxial-like approach to analyze the propagation characteristics of a hollow Gaussian beam (HGB) in the vicinity of its irradiance maximum in the plasma by taking note of the saturating character of the nonlinearities (i.e., ponderomotive, collisional, and relativistic). In continuation of previous investigations (Sodha *et al.*, 2009*a*, 2009*b*) Misra and Mishra (2009) modeled the propagation of a hollow Gaussian electro-magnetic beam in a plasma, considering the combined effect of relativistic and ponderomotive nonlinearity. It is shown that the critical curves and self focusing depend strongly on the order of the HGB; the propagation of the HGB follows the characteristic three regimes in the vicinity of the maximum irradiance. To our best knowledge, earlier theoretical investigations have tacitly considered beams with a Gaussian intensity distribution along the wavefront, implying that the laser is operated in the TEM_{00} mode. The aim of this article is to investigate, for the first time, the effect of a deviation from an initial Gaussian beam spot assumption on the actual evolution of the beam profile.

The physics of laser plasma interaction in the relativistic regime has been identified as an emerging area in the

Address correspondence and reprint requests to: A. Sharma, Centre for Plasma Physics, School of Mathematics & Physics, Queen's University Belfast, BT7 1NN Belfast, United Kingdom. E-mail: a_physics 2001@yahoo.com

recent few years, and is often referred to as high-field science. The high electric field associated with the propagation of extremely intense laser beams leads to a quiver speed of electrons on the order of the speed of light in vacuum, causing significant increase in the mass of electrons and a consequent increase in the dielectric constant of the plasma; this is one of the typical mechanisms resulting in the self-focusing of beam (Hora, 1975). Relativistic effects are dominant for a pulse duration shorter than the time needed for the manifestation of ponderomotive nonlinearity. Under the action of the ponderomotive force, electrons and ions move together at the ion sound speed c_s; thus, the characteristic time for the manifestation of the ponderomotive nonlinearity is r_0/c_s, where r_0 is the beam width. Additional phenomena contributing to the (de)focusing of an electromagnetic beam in a plasma are multiphoton (tunnel) ionization (Annou *et al.*, 1996), avalanche ionization (Stuart *et al.*, 1996; Derenzo *et al.*, 1974), harmonic generation (Sodha & Kaw, 1969), modification (Gurevich, 1978) of electron density, and nonlinear absorption (Sharma *et al.*, 2004). All these forms of nonlinearity are present and operate in various relative strengths in different regimes in terms of the irradiance, electron density, electron collision frequency, and duration of the pulse of the beam.

A laser beam is usually assumed to be characterized by a Gaussian intensity distribution function (*df*) along its wavefront. In contrast to this picture, Patel *et al.* (2005) measured the intensity profile for the Vulcan petawatt laser and found that only 20% of the energy was contained within the full-width-at-half-maximum (FWHM) of 6.9 μm and 50% within 16 μm. For comparison, a Gaussian *df* would contain 50% of the energy within the FWHM and 97.6% within 16 μm. Nakatsutsumi *et al.* (2008) recently suggested a *q*-Gaussian distribution function (Tsallis, 1988), namely:

$$f(r) = f(0)[1 + (r/4.4539\mu m)^2]^{-1.4748} \tag{1}$$

(see Fig. 1), to reproduce this behavior (here r is the spatial coordinate in the radial direction, and $f(0)$ is a real constant, to be determined by normalization requirements). Further investigations of the laser beam spot profile on the Vulcan laser in Rutherford Appleton laboratories (Davies, J.R. (2010). Private communication) seem to suggest that the beam intensity is characterized by a function of the form

$$f(r) = f(0)\left(1 + \frac{r^2}{qr_0^2}\right)^{-q}, \tag{2}$$

– cf. (1) above – or by a combination of such functions, where the values of the relevant parameters (q and r_0 here) can be obtained by fitting experimental data. Inspired by these challenging findings, we have here undertaken a thorough investigation of the spatial beam profile dynamics of a *q*-Gaussian laser beam propagating in relativistic plasma.

A few comments on nonthermal distributions appear to be in order here, for the sake of rigor and completeness. In fact, Ex. (1) is structurally reminiscent of the κ distribution (Vasyliunas, 1968; Hellberg *et al.*, 2009). (Various forms of the κ distribution have appeared in the past; we refer the reader to the discussion in the references by Hellberg *et al.* (2009) and Livadiotis and McComas (2009).) As pointed out above, it is also inspired by the Tsallis ("*q*-Gaussian") distribution (Tsallis, 1988), which lies in the foundation of non-extensive thermodynamics. Despite a number of works that have addressed the apparent ubiquity of the former (kappa) distributions in various plasma contexts (Treumann, 2001; Treumann *et al.*, 2004; Collier, 2004), there is at this stage no comprehensive theory relating this family of distributions to the fundamental underlying physics. Quite remarkably, a recent study (Livadiotis & McComas, 2009) claims to establish a rigorous link between the κ (family of) distribution(s) and the Tsallis distribution. This analogy is however certainly not algebraically straightforward, and still appears to be a controversial topic.

2. ANALYTICAL MODEL

The effective dielectric constant of a homogeneous plasma in the presence of a electromagnetic beam can be formally expressed as (Sodha *et al.*, 1976)

$$\epsilon = 1 - (\omega_p^2/\omega^2) + \phi(|E|^2), \tag{3}$$

where ω_p is the plasma frequency, ω is the frequency, and E is the electric field associated with the laser beam. The explicit dependence of the function ϕ on $|E|^2 = EE^*$ (the star here denoting the complex conjugate) needs to be determined in terms of the physical system considered. By increasing the beam power, the dielectric constant tends to reach its saturation value. The nonlinear character of the dielectric constant thus affects the dynamics of the laser beam and has naturally been attracting significant attention among researchers for well over 30 years. Some challenging aspects of the beam propagation characteristics are revealed by considering non-Gaussian beam behavior, as shown and discussed in the following. We shall investigate here the non-paraxial propagation characteristics of a petawatt (10^{15} W) laser beam with power 0.32 PW and intensity 1.37×10^{18} W/cm^2 with spatial and temporal resolution of 30 μm and 17 ps, respectively. The intensity distribution profile of the beam is considered to be given by a *q*-Gaussian function, in fact given by (1) above.

Let us consider a circularly polarized laser beam propagating in the axial (z-)direction:

$$E(r, z, t) = A(r, z, t)(e_x + ie_y)\exp[-i(\omega t - kz)], \tag{4}$$

where e_x and e_y are the unit vectors along the x and y axes, respectively. The amplitude A is a slowly varying function of space (r, z) and time t. The electric field E satisfies the wave equation

$$\nabla^2\mathbf{E} - \frac{\epsilon}{c^2}\frac{\partial^2\mathbf{E}}{\partial t^2} = 0, \tag{5}$$

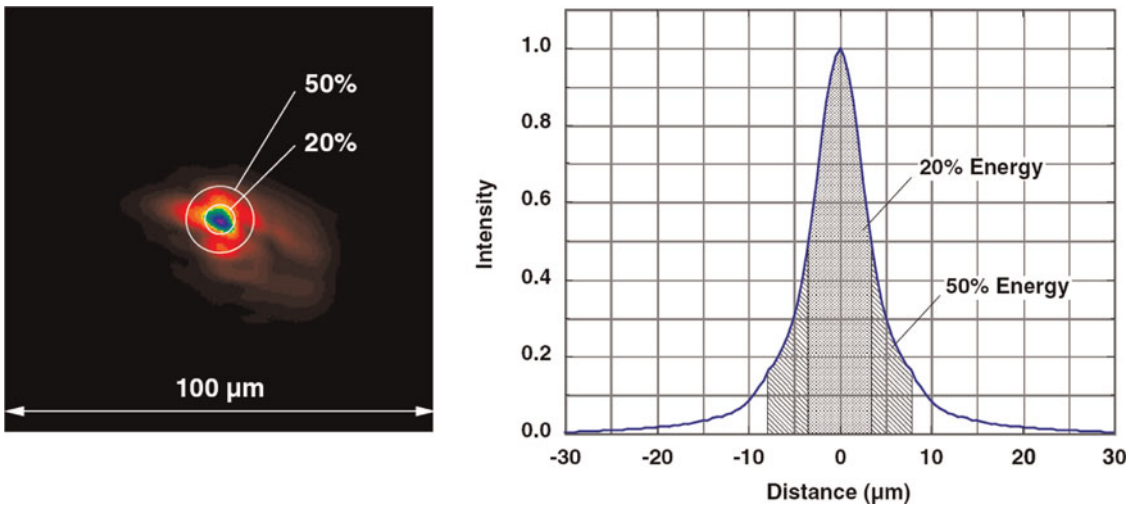

Fig. 1. (Color online) Image of focal spot *in vacuo* at low energy taken with a 16-bit CCD camera (**left**). Radial lineout of focal spot intensity showing 20% and 50% encircled energy boundaries (**right**). Adapted from (Patel *et al.*, 2005)

which can be directly derived from Maxwell's equations. For a transverse field **E**

$$\nabla \cdot \mathbf{E} = \mathbf{k} \cdot \mathbf{E} = 0, \tag{6}$$

k here being the propagation vector. We note that $\nabla(\nabla.\mathbf{E})$ has been neglected in deriving Eq. (5) (even if **E** has a longitudinal component, the term $\nabla(\nabla\cdot\mathbf{E})$ can be neglected provided that $\frac{c^2}{\omega^2}|\frac{1}{\epsilon}\nabla^2 ln\epsilon| \ll 1$, a condition satisfied in most cases of interest). We need to stress that (5) is a *nonlinear* equation, since ϵ depends on $|\mathbf{E}|$ *via* (3).

The initial intensity profile of the q-Gaussian laser pulse can be written as,

$$a^2(r, z = 0, t) = a_{00}^2\left(1 + \frac{r^2}{qr_0^2}\right)^{-q} F(t). \tag{7}$$

where $a = eA/m\omega c$ is the normalized laser field and a_{00} is the initial normalized laser field amplitude. We note that $a = 0.8510^{-9}\sqrt{I}\times\lambda$, where I is expressed in $\mathrm{W/cm^2}$ and λ is expressed in μm. We assume the temporal profile of the pulse—see $F(t)$ in Eq. (7)—to be Gaussian, viz.,

$$F(t) = \exp(-t^2/\tau_0^2). \tag{8}$$

where τ_0 is the initial pulse width. The deviation from the Gaussian profile is measured by the real parameter q, which acquires smaller (finite) values for a strongly non-Gaussian profile. The usual Gaussian distribution is recovered for $q \to \infty$. Note that the steady state dynamics is implicitly considered in order to explore the spatial evolution of a q-Gaussian beam profile.

Figure 2 illustrates the normalized intensity profile of the laser beam for different values of q. Small values of q are characterized by a long tail, while as q increases toward higher values, the distribution gradually converges to a Gaussian profile, attained at infinity.

The laser pulse propagates at the group velocity $v_g = c^2k/\omega$, where k is the wave number given by the plasma dispersion relation, $c^2k^2 = \omega^2 - \omega_p^2$. We shall introduce the coordinate transformation $\tau = t - (z/v_g)$ and $z \to z$. Now using Eq. (4), the wave Eq. (5) can be written as,

$$2ik\frac{\partial a}{\partial z} + \frac{\partial^2 a}{\partial r^2} + \frac{1}{r}\frac{\partial a}{\partial r} + \frac{\omega^2}{c^2}\epsilon(r, z, t)a = 0, \tag{9}$$

Eq. (9) is the equation of evolution for the field envelope, and includes the effects of diffraction, transverse focusing and nonlinearity. The last term represents the nonlinearity effect, which arises due to the dependence of the dielectric constant on the intense laser field.

The nonlinear dielectric constant appearing in Eqs. (5) and (9) may be expressed (in the non-paraxial approximation) as

$$\epsilon(r, z, t) = \epsilon_0(z, t) + r^2\epsilon_1(z, t) + r^4\epsilon_2(z, t), \tag{10}$$

where $\epsilon_1(z, t)$ and $\epsilon_2(z, t)$ express the radial spot profile dependence (vanishing at $r = 0$). The exact expansion for $\epsilon(r, z, t)$ will be obtained later; refer to Eqs. (21)–(24) below.

The solution of Eq. (9) can be expressed as

$$a(r, z, t) = a_0(r, z, t)\exp[-ikS(r, z, t)], \tag{11}$$

where both amplitude (a_0) and eikonal (S) are real quantities; eikonal S is related with the curvature of wavefront. Substituting for a from Eq. (11) in Eq. (9) and separating the real from the imaginary parts, one obtains

$$\frac{\partial a_0^2}{\partial z} + \frac{\partial S}{\partial r}\frac{\partial a_0^2}{\partial r} + a_0^2\left(\frac{\partial^2 S}{\partial r^2} + \frac{1}{r}\frac{\partial S}{\partial r}\right) = 0, \tag{12}$$

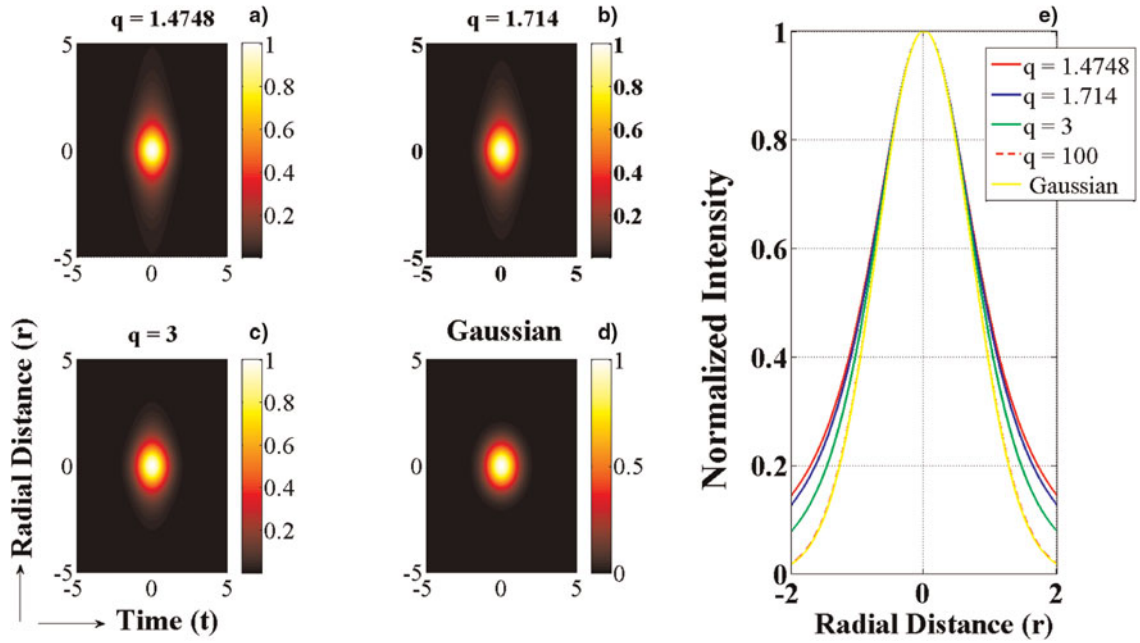

Fig. 2. (Color online) Initial intensity profile of the q-Gaussian laser pulse for $q = 1.4748$, 1.714, 3, and ∞; from (Eqs. 8 and 7). The radial distance (r) and time (t) are normalized by the initial beam width and initial pulse width respectively. Panels (**a**)–(**d**) show the normalized 3D intensity initial snapshots of a q-Gaussian laser pulse whose spatial beam radius (r_0) is 30 μm and temporal pulse duration (τ_0) is 17 ps, respectively. Figure 2e shows the spatial intensity profiles of q-Gaussian beam. The color bar represents the variation of the initial intensity. The long tail associated with small q is clearly visible.

and

$$2\frac{\partial S}{\partial z}+\left(\frac{\partial S}{\partial r}\right)^2=\frac{\omega^2\epsilon(r,z,t)}{c^2k^2}+\frac{1}{k^2a_0}\left(\frac{\partial^2 a_0}{\partial r^2}+\frac{1}{r}\frac{\partial a_0}{\partial r}\right). \quad (13)$$

Adopting the higher order paraxial theory (Liu & Tripathi, 2001; Sodha & Faisal, 2008; Sodha *et al.*, 1976, 1974), we anticipate a solution for Eqs. (12) and (13) in the form

$$a_0^2(r,z,t)=\frac{a_{00}^2}{f(z)^2}\left[1+\alpha_0\frac{r^2}{(r_0f(z))^2}+\alpha_2\frac{r^4}{(r_0f(z))^4}\right]\times\left[1+\frac{r^2}{q(r_0f(z))^2}\right]^{-q}F(t), \quad (14)$$

and

$$S(r,z,\tau)=\frac{r^2}{2f}\frac{df}{dz}+\frac{r^4}{r_0^4}S_2, \quad (15)$$

where α_0, α_2, S_2 and the beam width parameter f are functions of z. Identifying the components of the eikonal (S) in the latter expression, the first term above is indicative of the spherical curvature of the wavefront, while S_2 represents its departure from the spherical nature. The parameters α_0, and α_2 characterize the off-axis contribution to the beam intensity; these higher order terms play a crucial role in the dynamics of a q-Gaussian beam, as we shall show below. The latter two Eqs. (14) and (15) have also been employed by Liu & Tripathi (2001) and Sodha & Faisal (2008) for non-paraxial Gaussian beam propagation.

Using Eqs. (11), (14), and (15), the intensity profile of a q-Gaussian laser pulse can be expressed as

$$a^2(\rho,\zeta,\tau)=\frac{a_{00}^2F(\tau)R(0)^2}{R(\zeta)^2}\left[1+\alpha_0\frac{\rho^2}{R(\zeta)^2}+\alpha_2\frac{\rho^4}{R(\zeta)^4}\right]\times\left[1+\frac{\rho^2}{qR(\zeta)^2}\right]^{-q}\exp\left[-i\epsilon_0^{1/2}\frac{\rho^2}{R(\zeta)}\frac{dR(\zeta)}{d\zeta}-\frac{2\rho^4}{\rho_1^4}\tilde{S}_2\right], \quad (16)$$

where $R(\zeta)=\rho_1 f(\zeta)$ is the beam width (in the radial direction), $R(0)=\rho_1=r_0\omega/c$ is the initial dimensionless beam width [viz. $f(\zeta=0)=1$], $\zeta=\omega z/c$, $\rho=r\omega/c$ and $\tilde{S}_2=S_2\omega/c$. The laser pulse profile in plasma can be obtained by solving the following four coupled second order ordinary differential Eqs. (ODEs):

$$\epsilon_0(\zeta,\tau)\frac{d^2f}{d\zeta^2}=\frac{(1+8\alpha_2-3{\alpha_0}^2-2\alpha_0+4/q)}{\rho_1^4f^3}+\epsilon_1(\zeta,\tau), \quad (17)$$

$$\frac{d\tilde{S}_2}{d\zeta}=\frac{\rho_1^6\epsilon_2(\zeta,\tau)}{2}+\frac{1}{f^6}\left({\alpha_0}^3-{\alpha_0}^2-7\alpha_0\alpha_2+2\alpha_2+\frac{\alpha_0-1}{q}-\frac{3}{q^2}\right)-\frac{4\tilde{S}_2}{f}\frac{df}{d\zeta}, \quad (18)$$

$$\frac{d\alpha_0}{d\zeta}=-16\tilde{S}_2f^2, \quad (19)$$

and

$$\frac{d\alpha_2}{d\zeta} = \alpha_0 \frac{\partial \alpha_0}{\partial \zeta} - 8\alpha_0 \tilde{S}_2 f^2 + 8\tilde{S}_2 f^2, \tag{20}$$

where $p = a_{00}2\ F(\tau)/f(\zeta)^2$. At $\zeta = 0$ and $\tau = 0$, $p = a_{00}^2$ is the initial normalized laser field amplitude.

We have obtained Eqs. (17) and (18) by substituting (14), (15) [along with (10)] into (13), and then equating the coefficients of r^2 and r^4, respectively. In a similar fashion, Eqs. (19) and (20) were obtained by substituting (14) and (15) into (12). At this stage, knowing ϵ_0 and ϵ_1, one can solve the first three among the equations above and then integrate the latter one numerically, to obtain the beam width parameter (f) as a function of z. If the functional form of ϵ_1 is known, one can easily evaluate ϵ_0 and ϵ_1. Note that their form depends on (and reflects the physical features of) the beam-plasma model considered (Sodha & Faisal, 2008; Sodha *et al.*, 1976, 1974).

The index of refraction for a small-amplitude electromagnetic wave (a weak laser beam) propagating in plasma with density n_e is given by $n = ck/\omega = (1-\omega_p^2/\omega^2)^{1/2}$. As the laser intensity increases, the effect of the transverse quiver motion of plasma electrons becomes stronger and the electron mass is modified by the relativistic effect, *viz.* $\omega_p^2 \rightarrow \omega_p^2/\gamma$, which eventually affects the expression for n. The conservation of transverse canonical momentum imposes $a = \gamma\beta$, where $\beta = v/c$ is the normalized velocity of the plasma electrons, and the Lorentz factor γ (for the electrons) is given by $\gamma \approx (1+a^2)^{1/2}$ for a circularly polarized laser [read $(1+a^2/2)^{1/2}$ for linear polarization]. Thus, the relativistic refractive index of plasma can be written as $n = [1-(\omega_{p0}^2/\omega^2)(1+a^2)^{-1/2}]^{1/2}$, where ω_{p0} is the unperturbed plasma frequency (in the absence of the electromagnetic field).

If the radial profile of γ attains a maximum on the axis, i.e., for a laser beam intensity profile peaked on the axis, or $\gamma(0) > \gamma(r)$, then the index of refraction $n(r)$ can reach a maximum on the axis. This causes the wavefront to curve inwards and the laser beam to converge, which may result in optical guiding of the laser light. Since the laser phase velocity v_{ph} depends on the index of refraction, $v_{ph} = c/n$, it will then depend on the laser intensity. Local variation in the phase velocity will modify the shape of the laser pulse, and, consequently, the spatial and temporal profile of the laser intensity. Relativistic self-focusing occurs when the laser power exceeds a critical power, given by $P_c = 17(\omega/\omega_p)^2$ GW. On the other hand, photoionization can defocus light and thus increase the self-focusing threshold, by increasing the on-axis density and refractive index. When this focusing effect just balances the defocusing due to diffraction, the laser pulse can be self-guided, and thus propagate over a long distance with high intensity. For a laser with peak intensity along the axis, this requires the relationships $\partial(a^2)/\partial r < 0$ and $\partial n/\partial r < 0$ to be satisfied for relativistic guiding. In the following, a circularly polarized laser is assumed (it is nevertheless straightforward to extend the formalism to a linearly polarized beam).

A general expression of the relativistic dielectric constant ($\epsilon = n^2$) of plasma for a large amplitude electromagnetic wave can be written as

$$\epsilon = 1 - (\omega_{p0}^2/\omega^2)(1+a^2)^{-1/2}. \tag{21}$$

Introducing a q-dependent field distribution (as given by Eq. (16)) in the latter Eq. (21), one obtains the components of the dielectric constant in (10) as

$$\epsilon_0(\zeta, \tau) = 1 - (\omega_{p0}^2/\omega^2)(1+p)^{-1/2}, \tag{22}$$

and

$$\epsilon_1(\zeta, \tau) = -(1/2)\ (1-\alpha_0)\frac{\omega_{p0}^2}{\omega^2} p(1+p)^{-3/2}\frac{1}{R^2(\zeta)}, \tag{23}$$

and

$$\epsilon_2(\zeta, \tau) = -\frac{\omega_{p0}^2}{\omega^2}\left[\frac{3}{8}\frac{p(1-\alpha_0)^2}{(1+p)^2} - \frac{1}{2}\frac{(\alpha_2 - \alpha_0 + \frac{1}{2(1+q^{-1})})}{(1+p)}\right] \times p(1+p)^{-1/2}\frac{1}{R^4(\zeta)}. \tag{24}$$

The critical relation relating the beam width and the beam power, as can be derived from Eqs. (17) and (23), will feature a parametric dependence on q. For $d^2f/d\zeta^2 = 0$ at $\zeta = 0$, $\tau = 0$, ($\alpha_0 = 0$ and $\alpha_2 = 0$) one obtains

$$\rho_1^2 = \frac{2(1+4/q)(1+a_{00}^2)^{3/2}}{a_{00}^2(\omega_{p0}^2/\omega^2)}, \tag{25}$$

which for infinite q recovers the expression derived earlier for a Gaussian beam in non-absorbing collisional plasma (Sharma *et al.*, 2003). Eq. (25) expresses the dimensionless beam width ρ_1 (at $f = 1$) as a function of the (reduced) laser field amplitude a_{00} and thus related to the initial beam power. The function can be depicted on the (a_{00}, ρ_0) plane and is generally referred to as the critical power curve or, simply, the *critical curve*. If the initial values of a_{00} and ρ_1 of a laser beam are such that the point (a_{00}, ρ_0) lies on the critical curve, the value of $d^2f/d\zeta^2$ will vanish at $\xi = 0$ ($z = 0$). Since the initial value of $df/d\zeta$ (in case the wave front is plane) is zero, the value of $df/d\zeta$ continues to be zero as the beam propagates through the plasma. Hence, the initial value of f, which is unity (at $z = 0$), will remain unchanged. The beam thus propagates without any change in its beam width. This regime is known as uniform waveguide propagation. If an initial point (a_{00}, ρ_0), corresponding to the initial ($z = 0$) normalized laser field amplitude and beam radius, lies below the critical curve (that is, on the same side of the curve as the origin) then

$d^2f/d\zeta^2 > 0$, while if a point lies on the other side of the critical curve then $d^2f/d\zeta^2 < 0$. We retain that, when the initial point lies below (above) the critical curve, the beam width parameter will increase (decrease, respectively) at $(z, f) = (0, 1)$.

Figure 3 illustrates the dependence of the critical curves on the value of q. The critical curves are down-shifted as q increases because of enhanced nonlinearity. The critical curves for the homogeneous and inhomogeneous cases remain the same, since these are dependent on the magnitude of the parameters at $z = 0$; since $\alpha_0 = \alpha_2 = 0$ at $z = 0$, the higher order terms do not affect the critical curves. As a matter of fact, the critical curves (at $z = 0$) are not relevant in inhomogeneous plasma, in which case the inhomogeneity parameters increase with the value of z. To see this, we recall that the higher order terms (α_0, α_2 and S_2) in the non-paraxial beam propagation are functions of z and in fact vary as the beam propagates in the plasma. Physically, these higher order terms represent the medium inhomogeneity in z; however, the critical relation is derived at $z = 0$, where these terms vanish.

The critical curves remain the same as in paraxial beam propagation (Sharma *et al.*, 2008) as z increases, due to the plasma parameter variation (higher order terms or inhomogeneity parameters). The critical beam power and beam width relation (as given by Eq. (25)) shows the inverse dependence of the initial beam radius on the q-factor. This relationship between the critical beam power and the beam width explains clearly the beam convergence (or divergence) of a q-Gaussian electromagnetic beam. We also see from Figure 3 that the minimum value of ρ_1 is higher for lower q-values (i.e., for a larger deviation from the Gaussian). It is thus predicted that larger spot-size beams with lower q-values can be relativistically guided in a plasma, in comparison with smaller spot-size Gaussian beams (or, e.g., q-Gaussian ones with large q value).

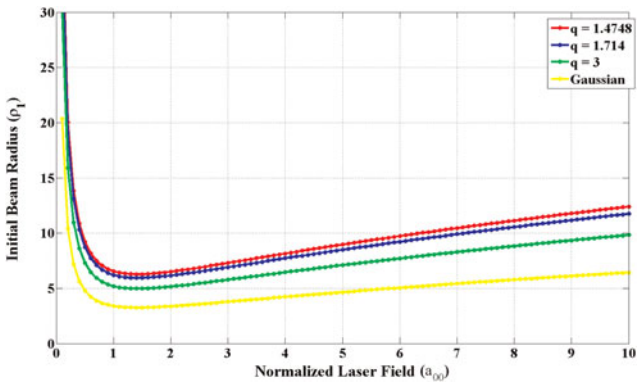

Fig. 3. (Color online) The initial (at $\zeta = 0$) dimensionless beam width (ρ_1) is depicted *versus* the normalized laser field (a_{00}) for different values of the q-parameter. The relation between the (ρ_1) and (a_{00}) is expressed by Eq. (25). The beam propagation corresponding to points (a_{00}, ρ_1) which lie on these curves (critical curve) leads to relativistic guided uniform beam propagation.

3. NUMERICAL INVESTIGATION

The evolution of a q-Gaussian beam profile can be analyzed by numerically by solving the ODE (17) coupled with Eqs. (18–20). Eqs. (17) can be numerically integrated using appropriate boundary conditions to evaluate the beam width parameter f as a function of z. For an unperturbed initial plane wave, the boundary conditions on Eq. (17) were taken as: $f = g = 1$, and $d f/d\zeta = 0$ at $\zeta = 0$. We have performed a numerical computation for the following laser plasma parameters $a_{00} = 0.1$ ($I_0 = 1.37 \times 10^{16}$ W/cm^2, $\lambda = 1$ μm), $r_0 = 30$ μm, $n_0 = 4 \times 10^{20}$ cm^{-3} and $\omega = 10^{15}$ rad sec^{-1}.

We have numerically obtained the normalized q-Gaussian beam intensity profile $a^2(\rho, \zeta, \tau)$, as given by Eq. (16), initially (at $T_1 = 0$) and then at given propagation time (equivalent to a given propagation distance), as the beam propagates in the plasma. The results are shown in Figure 4 at propagation time instants $T_2 = 2$ ns, $T_3 = 5$ ns, and $T_4 = 9$ ns, for various values of q. The propagation time $T = \zeta/c$ (proportional to the propagation distance z or ζ) advances from left to right (within a given row, for given q). The top row (see Figs. 4a to 4d) depicts the intensity profile for a q-Gaussian beam (for $q = 1.4748$) propagating through relativistic plasma, in the nonparaxial region, at instants T_1, T_2 and T_3. The second, third, and bottom rows (see Figs. 4a to 4d, 4e to 4h, and 4i to 4l, respectively) show the variation of the normalized intensity for higher q values (closer to a Gaussian *df*) at the same time instants as the top column. We witness a fast focusing of the laser beam in the nonparaxial region. Transverse focusing of the beam dominates over diffraction, due to the nonlinear effect of relativistic mass variation. The difference in focusing/defocusing of the axial and off-axial rays leads to the beam profile maximum actually splitting on the plane transverse to propagation.

It is obvious that in the paraxial region, the intensity of the laser beam is maximum at $r = 0$ along the distance of propagation as $\alpha_0 = \alpha_2 = 0$. While in the nonparaxial region the laser intensity becomes minimum at $r = 0$, it assumes a ring structure or a split beam-maximum profile (Sodha & Faisal, 2008). In Eq. 18 at $z = 0$, $dS_2/d\zeta$ is positive and α_0 starts decreasing, while α_2 increases sharply with the increase in z. Due to the combined effect of α_0 and α_2 the laser intensity acquires a minimum on the axis and the intensity of the nonparaxial region increases. Focusing becomes faster in the nonparaxial case in comparison to the paraxial case due to the participation of the off-axis components ($\alpha_2 \neq \alpha_2 \neq 0$). For higher q (see the bottom row in Fig. 4), the behavior is essentially tantamount to that of a Gaussian beam (Liu & Tripathi, 2001; Sodha & Faisal, 2008; Sharma & Chauhan, 2008). Comparing the right-end panels—cf. Figs. 4(d, h, l, p)—we see that the focused beam intensity decreases as the value of q increases (top to bottom row, in the plot). The simulation results clearly suggest an intensity amplification by a factor 80 or higher, for a q-Gaussian (for $q = 1.4748$)

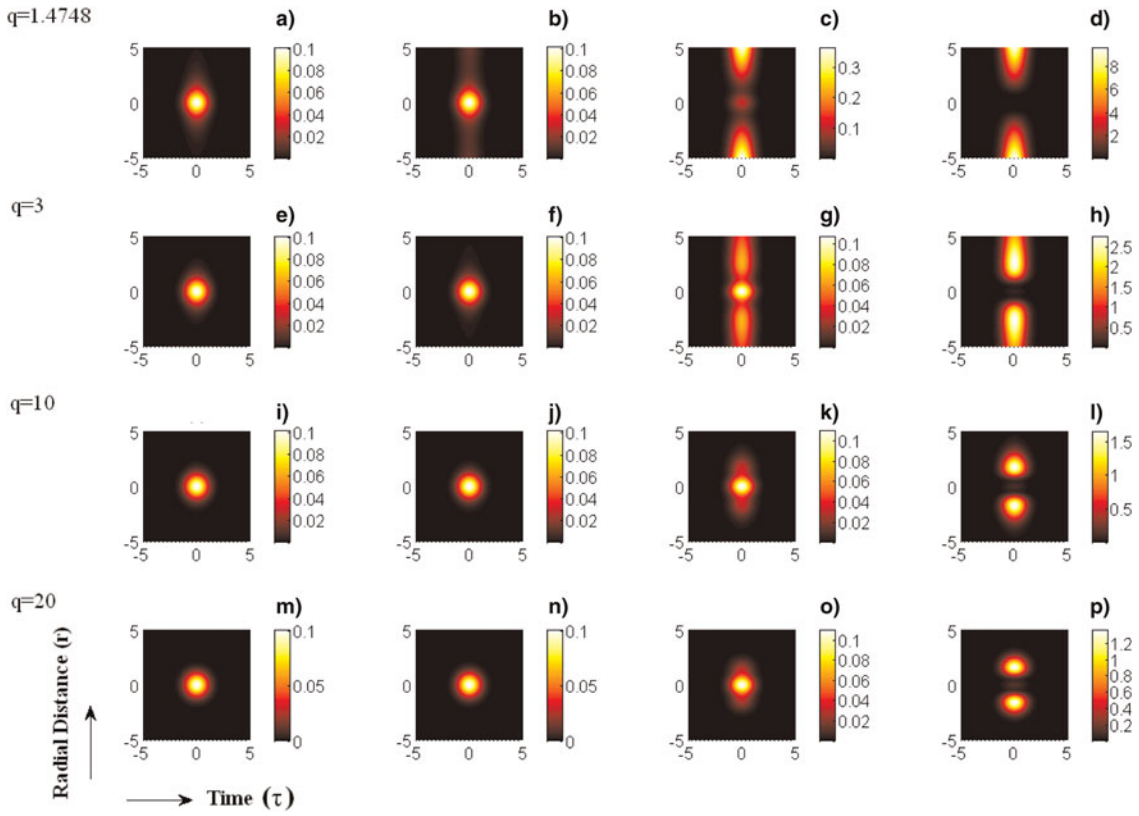

Fig. 4. (Color online) Spatial evolution of a q-Gaussian circularly polarized laser beam: the variation of the normalized intensity, as obtained from Eqs. (8) and (16), with radial distance r and time t is shown at different propagation time (equivalent to fixed propagation distance): at $T_1 = 0$ (first column); $T_2 = 3$ fs (second column); $T_3 = 7$ fs (third column); $T_4 = 10$ fs (fourth column) (corresponding to propagation distance $\zeta = 0$, 18 μm, 45 μ and 81 μm). The radial distance (r) and time (t) are normalized by the initial beam width and initial pulse width respectively. The results are shown for different q values: $q = 1.4748$ (value as in Patel *et al.* (2005); top row); 3 (second row); 10 (third row); 20 (practically Gaussian; bottom row). The laser plasma parameters used in the computation are: $a_{00} = 0.1$ ($I_0 = 1.37 \times 10^{16}$ W/cm^2, $\lambda = 1$ μm), $r_0 = 30$ μm, $\tau_0 = 17$ ps, $n_0 = 4 \times 10^{20}$ cm^{-3} and $\omega = 10^{15}$ rad sec^{-1}. The color bar represents the variation of the normalized intensity.

petawatt laser beam in femtosecond time duration, compared to a Gaussian beam of the same other characteristics.

We see in Figure 4 that the divergence of the axial rays is stronger than that of the off-axial ones. The intensity distribution thus acquires a ring or split beam-maximum shape. The coefficients α_0 and α_2 characterizing the non-Gaussian shape start to grow with time (or propagation distance). Considering (in Fig. 4) a laser intensity $I_0 = 1.37 \times$

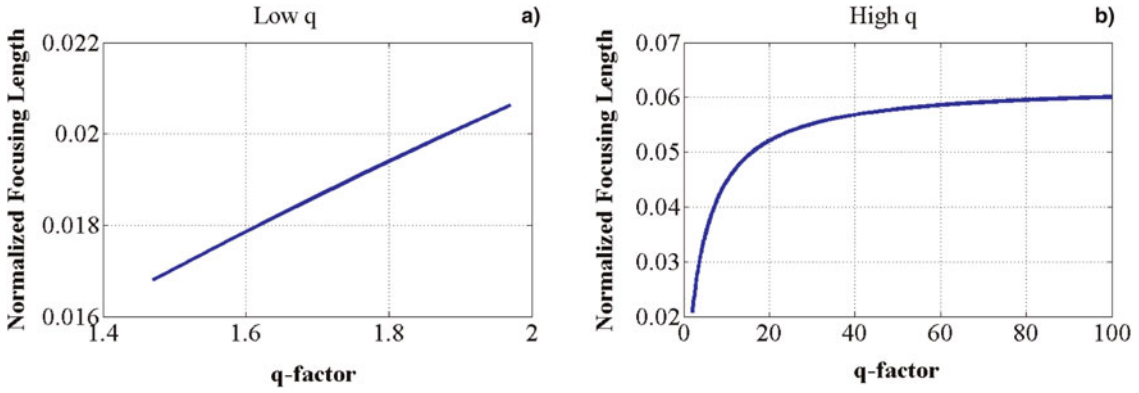

Fig. 5. (Color online) The dependence of the normalized focusing length on the non-Gaussianity parameter q is depicted. The focusing length ($\rho_1 \omega / \omega_{p0} \sqrt{2}$) is normalized by the diffraction length (kr_0^2). The laser-plasma parameters used for the numerical computation are the same as in Figure 4.

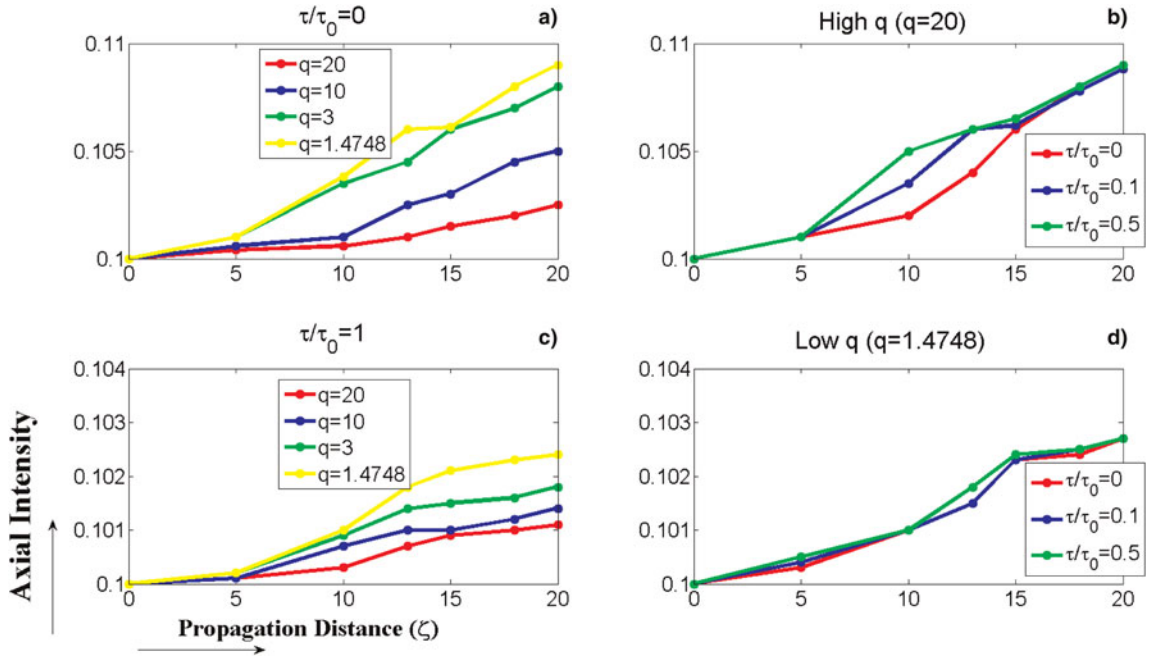

Fig. 6. (Color online) Dependence of axial intensity $a^2(\rho = 0, \zeta, \tau)$ on the propagation distance (ζ). Panels (**a**) and (**c**) show the variation of the axial intensity with ζ for different values of the non-Gaussian parameter (q) at $\tau/\tau_0 = 0$ and $\tau/\tau_0 = 1$. Panels (**b**) and (**d**) show the variation in the axial intensity along ζ at various values of time, for high and low values of the non-Gaussian parameter q. The laser-plasma parameters used for the numerical computation are the same as in Figure 4.

10^{16} W/cm^2 and an electron density $n_0 = 4 \times 10^{20}$ cm^{-3}, at $T_4 = 9$ ns (equivalent to $z = 81$ μm), $\alpha_2 > 1$, we see that the laser pulse intensity becomes minimal on the axis and acquires a ring-like structure at some time (distance). This ring formation or beam splitting effect was earlier pointed out (Liu & Tripathi, 2001; Sodha & Faisal, 2008; Sharma & Chauchan, 2008). This effect has been observed experimentally by Chessa *et al.* (1999), who observed a ring-shaped distribution of the Gaussian laser pulse for intensity $I_0 = 6 \times 10^{17}$ W/cm^2, and electron density $n_0 \sim 10^{20}$ cm^3, at $z \sim 280$ μm. Most interestingly, this effect appears in fact to be intensified for non-Gaussian beams, in comparison to Gaussian ones (compare the upper three panels to the bottom one, in Fig. 4.)

We have numerically solved the coupled Eqs. (17)–(20) for the beam width parameter f, the eikonal component S_2, and the nonparaxial parameters (a_0 and a_2), to evaluate the focusing length of the beam. The numerical computation depicts the dependence of the focusing length on the non-Gaussianity parameter q. In Figure 5, the normalized self-focusing length is plotted over a range of q values. Here we have scaled the focusing length ($\rho_1 \omega/\omega_{p0}\sqrt{2}$) by the diffraction length (kr_0^2). The self-focusing length in the plasma (i.e., the minimum propagation length in the plasma where the beam becomes focused and the beam radius attains its minimum value (cf. Fig. 1b in Sharma *et al.*, 2008)), increases linearly for lower q values, as illustrated in Figure 5a. Figure 5b shows the dependence of the normalized focusing length on higher q-values. The simulation results demonstrate a saturating nature, as q increases toward ∞. It can be seen from Figure 2 that the higher the value of q, the narrower the beam becomes.

In order to demonstrate the temporal dependence of the beam irradiance, we have evaluated the axial intensity ($a^2(\rho = 0, \zeta, \tau)$) as a function of ζ (distance of propagation). We have numerically solved Eq. (16) along $\rho = 0$, together with Eqs. (17)–(20) for the typical values of laser-plasma parameters as used in Figure 4. The dependence of the axial intensity on the propagation distance (ζ) is shown in Figure 6. Parts 6a, 6c show the variation of the axial intensity with ζ for different values of the non-Gaussian parameter (q) at $\tau/\tau_0 = 0$ and at $\tau/\tau_0 = 1$ respectively. Figures 6b, 6d depict the variation of the axial intensity along ζ at various time instants, for high and low values of the non-Gaussian parameter (q), respectively. These results (6a-6d)) predict a very small variation in axial intensity of beam at temporal axis (at $\tau/\tau_0 = 0$) as well as at off-temporal axis (at $\tau/\tau_0 \neq 0$) for a range of q values. Figure 6 also confirms our earlier result (as shown by Fig. 4) that there is no significant variation of axial intensity (at $\tau/\tau_0 \neq 0$).

4. CONCLUSIONS

In conclusion, we have investigated the spatial evolution of a non-Gaussian circularly polarized beam propagating through relativistic plasma. A q-Gaussian distribution function was adopted for the beam spot profile. We have shown that the beam intensity profile converges toward a split profile due

to the off-axis field contribution to relativistic nonlinear terms, as the beam propagates through the plasma. The difference in focusing/defocusing of the axial and co-axial rays leads to the formation of a split beam profile characterized by a minimum intensity on the axis and a maximum off it. Earlier theoretical and experimental results on Gaussian beam focusing and ring formation (Liu & Tripathi, 2001; Sodha & Faisal, 2008; Sharma & Chauchan, 2008; Chessa *et al.*, 1999) are thus confirmed, and extended to q-Gaussian laser beam spots. The beam-splitting effect seems to be intensified by a departure from a Gaussian beam spot profile.

We have numerically investigated the focusing of a q-Gaussian petawatt laser ($I_0 = 1.37 \times 10^{16}\,\mathrm{W/cm^2}$) and have obtained an increased beam intensity (for $q = 1.4748$). It is remarkable that the intensity of the final (focused) beam spot is lower for a Gaussian beam profile (i.e., for high q values). We also see that the self-focusing length of a non-Gaussian beam (low q values) is considerably lower than that of a Gaussian one, suggesting that deviation from a Gaussian behavior enhances self-focusing significantly.

Our results are of relevance in various contexts of beam plasma physics. Besides of the obvious relevance to inertial fusion, the ultra-high intensity laser channels in relativistic plasmas can have many other applications where localized electromagnetic fields are required. Our analytical and numerical results on the non-paraxial propagation of q-Gaussian beam in relativistic plasma can serve as a guide for experimental and numerical investigations of petawatt laser channeling in underdense plasmas. This should expand current knowledge in the fast ignition, high energy X-ray radiography and high energy density physics research. Petawatt lasers (power $\simeq 10^{15}$ W) focused to a few microns' region have proven to be useful tools for the study of high energy density physics (Board, 2003). Conditions comparable to those in stars, supernova remnants and other astrophysical objects can now be achieved in the laboratory and such lasers are employed in inertial confinement fusion schemes (Tabak *et al.*, 1994; Campbell *et al.*, 2006).

ACKNOWLEDGMENTS

This work was supported by a UK EPSRC Science and Innovation Award to the Center for Plasma Physics, Queen's University Belfast (Grant no EP/D06337X/1). J.R. Davies (IST, Lisbon, Portugal) is warmly acknowledged for providing access to a significant amount of inspiring data.

REFERENCES

Annou, R., Tripathi, V.K. & Srivastava, M.P. (1996). Plasma channel formation by short pulse laser. *Phys. Plasmas* **3**, 1356–1359.

Askaryan, G.A. (1962). Interaction between laser radiation and oscillating surfaces. *Sov. Phys. JETP* **15**, 1161–1162.

Board of Physics and Astronomy (2003). *Frontiers in High Energy Density Physics: The X–Games of Contemporary Science*. Washington, DC: National Academies Press.

Borisov, A.B., Borovskiy, A.V., Shiryaev, O.B., Korobkin, V.V., Prokhorov, A.M., Solem, J.C., Luk, T.S., Boyer, K. & Rhodes, C.K. (1992). Relativistic and charge–displacement self–channeling of intense ultrashort laser pulses in plasmas. *Phys. Rev. A* **45**, 5830–5845.

Campbell, E.M., Freeman, R.R. & Tanaka, A.K. (2006). Fast ignition inertial fusion: an introduction and preview. *Fusion Sci. Technol.* **49**, 249–253.

Chessa, P., Wispelaere, E. De, Dorchies, F., Malka, V., Marques, J.R., Hamoniaux, G., Mora, P. & Amiranoff, F. (1999). Temporal and angular resolution of the ionization–induced refraction of a short laser pulse in helium gas. *Phys. Rev. Lett.* **82**, 552–555.

Collier, M.R. (2004). Are magnetospheric suprathermal particle distributions inconsistent with maximum entropy considerations? *Adv Space Res.* **33**, 2108–2112.

Derenzo, S.E., Mast, T.S., Zaklad, H. & Muller, R.A. (1974). Electron avalanche in liquid xenon. *Phys. Rev. A* **9**, 2582–2591.

Deutsch, C., Bret, A., Firpo, M.C., Gremillet, L., Lefebvre, E. & Lifschitz, A. (2008). Onset of coherent electromagnetic structures in the relativistic electron beam deuterium–tritium fuel interaction of fast ignition concern. *Laser Part. Beams* **26**, 157–165.

Faenov, A.Yu., Magunov, A.I., Pikuz, T.A., Skobelev, I.Yu., Gasilov, S.V., Stagira, S., Calegari, F., Nisoli, M., De Silvestri, S., Poletto, L., Villoresi, P. & Andreev, A.A. (2007). X–ray spectroscopy observation of fast ions generation in plasma produced by short low–contrast laser pulse irradiation of solid targets. *Laser Part. Beams* **25**, 267–275.

Faure, J., Glinec, Y., Pukhov, A., Kiselev, S., Gordienko, S., Lefebvre, E., Rousseau, J.P., Burgy, F. & Malka, V. (2004). A laser–plasma accelerator producing monoenergetic electron beams. *Nature (London)* **431**, 541–544.

Geddes, C.G., Toth, C.S., Tilborg, J. Van, Esarey, E., Schroeder, C.B., Bruhwiler, D., Nieter, C., Cary, J. & Leemans, W.P. (2004). High quality electron beams from a laser wakefield accelerator using plasma–channel guiding. *Nature (London)* **431**, 538–541.

Gordon, D., Tzeng, K.C., Clayton, C.E., Dangor, A.E., Malka, V., Marsh, K.A., Modena, A., Mori, W.B., Muggli, P., Najmudin, Z., Neely, D., Danson, C. & Joshi, C. (1998). Observation of electron energies beyond the linear dephasing limit from a laser–excited relativistic plasma wave. *Phys. Rev. Lett.* **80**, 2133–2136.

Gurevich, A.V. (1978). *Nonlinear Phenomena in the Ionosphere*. Springer-Verlag: Berlin.

Hellberg, M.A., Mace, R.L., Baluku, T.K., Kourakis, I. & Saini, N.S. (2009). Comment on Mathematical and physical aspects of Kappa velocity distribution. *Phys. Plasmas* **16**, 094701–094705.

Hora, H. (1975). Theory of relativistic self–focusing of laser radiation in plasmas. *J. Opt. Soc. Am.* **65**, 882–886.

Hora, H. (2007). New aspects for fusion energy using inertial confinement. *Laser Part. Beams* **25**, 37–45.

Joshi, C., Malka, V., Darrow, C.B., Danson, C., Neely, D. & Walsh, F.N. (2002). Electron acceleration from the breaking of relativistic plasma waves. *Nature (London)* **377**, 606–608.

Kline, J.L., Montgomery, D.S., Rousseaux, C., Baton, S.D., Tassin, V., Hardin, R.A., Flippo, K.A., Johnson, R.P., Shimada,

T., Yin, L., Albright, B.J., Rose, H.A. & Amiranoff, F. (2009). Investigation of stimulated Raman scattering using a short–pulse diffraction limited laser beam near the instability threshold. *Laser Part. Beams* **27**, 185–190.

Lifschitz, A.Z., Faure, J., Glinec, Y., Malka, V. & Mora, P. (2006). Proposed scheme for compact GeV laser plasma accelerator. *Laser Part. Beams* **24**, 255–259.

Litvak, A.G. (1969). Finite-amplitude wave beams in a magnetoactive plasma. *Sov. Phys. JETP* **30**, 344.

Liu, C.S. & Tripathi, V.K. (2001). Self-focusing and frequency broadening of an intense short–pulse laser in plasmas. *J. Opt. Soc. Am. A* **18**, 1714–1718.

Livadiotis, G. & Mccomas, D.J. (2009). Beyond kappa distributions: Exploiting Tsallis statistical mechanics in space plasmas. *J. Geophys. Res.* **114**, A11105–A11125.

Malka, V., Fritzler, S., Lefebvre, E., Aleonard, M.M., Burgy, F., Chambaret, J.P., Chemin, J.F., Krushelnick, K., Malka, G., Mangles, S.P.D., Najmudin, Z., Pittman, M., Rousseau, J.P., Scheurer, J.N., Walton, B. & Dangor, A.E. (2002). Electron acceleration by a wake field forced by an intense ultrashort laser pulse. *Science* **298**, 1596–1600.

Mangles, S.P.D., Murphy, C.D., Najmudin, Z., Thomas, A.G.R., Collier, J.L., Dangor, A.E., Divall, E.J., Foster, P.S., Gallacher, J.G., Hooker, C.J., Jaroszynski, D.A., Langley, A.J., Mori, W.B., Norreys, P.A., Tsung, F.S., Viskup, R., Walton, B.R. & Krushelnick, K. (2004). Monoenergetic beams of relativistic electrons from intense laser-plasma interactions. *Nature (London)* **431**, 535–538.

Max, C.E., Arons, J. & Langdon, A.B. (1974). Self-modulation and self-focusing of electromagnetic waves in plasmas. *Phys. Rev. Lett.* **33**, 209–212.

Misra, S. & Mishra, S.K. (2009). Focusing of dark hollow Gaussian electromagnetic beam in a plasma with relativistic–pondermotive regime. *Progr. Electromagnetic Res. B* **16**, 291–309.

Modena, A., Najmudin, Z., Dangor, A.E., Clayton, C.E., Marsh, K.A., Monot, P., Auguste, T., Gibbon, P., Jakober, F., Mainfray, G., Dulieu, A., Louis-Jacquet, M., Malka, G. & Miquel, J.L. (1995). Experimental demonstration of relativistic self–channeling of a multiterawatt laser pulse in an underdense plasma. *Phys. Rev. Lett.* **74**, 2953–2956.

Nakajima, K., Fisher, D., Kawakubo, T., Nakanishi, H., Ogata, A., Kato, Y., Kitagawa, Y., Kodama, R., Mima, K., Shiraga, H., Suzuki, K., Yamakawa, K., Zhang, T., Sakawa, Y., Shoji, T., Nishida, Y., Yugami, N., Downer, M. & Tajima, T. (1995). Observation of ultrahigh gradient electron acceleration by a self–modulated intense short laser pulse. *Phys. Rev. Lett.* **74**, 4428–4431.

Nakatsutsumi, M., Davies, J.R., Kodama, R., Green, J.S., Lancaster, K.L., Akli, K.U., Beg, F.N., Chen, S.N., Clark, D., Freeman, R.R., Gregory, C.D., Habaral, H., Heathcote, R., Hey, D.S., Highbarger, K., Jaanimagi, P., Key, M.H., Krushelnick, K., Ma, T., Macphee, A., Mackinnon, A.J., Nakamura, H., Stephens, R.B., Storm, M., Tampo, M., Theobald, W., Woerkom, L.Van., Weber, R.L., Wei, M.S., Woolsey, N.C. & Norreys, P.A. (2008). Space and time resolved measurements of the heating of solids to ten million kelvin by a petawatt laser. *New J. Phys.* **10**, 043046–043058.

Patel, P.K., Key, M.H., Mackinnon, A.J., Berry, R., Borghesi, M., Chambers, D.M., Chen, H., Clarke, R., Damian, C., Eagleton, R., Freeman, R., Glenzer, S., Gregori, G., Heathcote, R., Hey, D., Izumi, N., Kar, S., King, J., Nikroo, A., Niles, A., Park, H.S., Pasley, J., Patel, N., Shepherd, R., Snavely, R.A., Steinman, D., Stoeckl, C., Storm, M., Theobald, W., Town, R., Van Maren, R., Wilks, S.C. & Zhang, B. (2005). Integrated laser–-target interaction experiments on the RAL petawatt laser. *Plasma Phys. Cont. Fusion* **47**, B833–B840.

Romagnani, L., Borghesi, M., Cecchetti, C.A., Kar, S., Antici, P., Audebert, P., Bandhoupadjay, S., Ceccherini, F., Cowan, T., Fuchs, J., Galimberti, M., Gizzi, L.A., Grismayer, T., Heathcote, R., Jung, R., Liseykina, T.V., Macchi, A., Mora, P., Neely, D., Notley, M., Osterholtz, J., Pipahl, C.A., Pretzler, G., Schiavi, A., Schurtz, G., Toncian, T., Wilson, P.A. & Will, O. (2008). Proton probing measurement of electric and magnetic fields generated by ns and ps laser-matter interactions. *Laser Part. Beams* **26**, 241–248.

Roth, M., Cowan, T.E., Key, M.H., Hatchett, S.P., Brown, C., Fountain, W., Johnson, J., Pennington, D.M., Snavely, R.A., Wilks, S.C., Yasuike, K., Ruhl, H., Pegoraro, F., Bulanov, S.V., Campbell, E.M., Perry, M.D. & Powell, H. (2001). Fast ignition by intense laser-accelerated proton beams. *Phys. Rev. Lett.* **86**, 436–439.

Seifter, A., Kyrala, G.A., Goldman, S.R., Hoffman, N.M., Kline, J.L. & Batha, S.H. (2009). Demonstration of symcaps to measure implosion symmetry in the foot of the NIF scale 0.7 hohlraums. *Laser Part. Beams* **27**, 123–127.

Sharma, A., Kourakis, I. & Sodha, M.S. (2008). Propagation regimes for an electromagnetic beam in magnetized plasma. *Phys. Plasmas* **15**, 103103–103109.

Sharma, A., Prakash, G., Verma, M.P. & Sodha, M.S. (2003). Three regimes of intense laser beam propagation in plasmas. *Phys. Plasmas* **10**, 4079–4084.

Sharma, A., Verma, M.P. & Sodha, M.S. (2004). Self-focusing of electromagnetic beams in collisional plasmas with nonlinear absorption. *Phys. Plasmas* **11**, 4275–4279.

Sharma, R.P. & Chauhan, P.K. (2008). Nonparaxial theory of cross-focusing of two laser beams and its effects on plasma wave excitation and particle acceleration: Relativistic case. *Phys. Plasmas* **5**, 063103–063108.

Singh, R., Sharma, A.K. & Tripathi, V.K. (2010). Relativistic self distortion of a laser pulse and ponderomotive acceleration of electrons in an axially inhomogeneous plasma. *Laser Part. Beams* doi:10.1017/S0263034610000200.

Sodha, M.S. & Faisal, M. (2008). Propagation of high power electromagnetic beams in overdense plasmas: Higher order paraxial theory. *Phys. Plasmas* **15**, 033102–033105.

Sodha, M.S. & Kaw, P.K. (1969). Theory of generation of harmonics and combination frequencies in a plasma. *Adv. Electron. Electron Phys.* **27**, 187–293.

Sodha, M.S., Ghatak, A.K. & Tripathi, V.K. (1974). *Self-Focusing of Laser Beams in Dielectric Plasmas and Semiconductors*. Delhi: India: Tata–McGraw–Hill.

Sodha, M.S., Ghatak, A.K. & Tripathi, V.K. (1976). Self focusing of laser beams in plasmas and semiconductors. *Prog. Opt.* **13**, 169–265.

Sodha, M.S., Mishra, S.K. & Misra, S. (2009*a*). Focusing of dark hollow Gaussian electromagnetic beams in a plasma. *Laser Part. Beams* **27**, 57–68.

Sodha, M.S., Mishra, S.K. & Misra, S. (2009*b*). Focusing of dark hollow Gaussian electromagnetic beams in a magnetoplasma. *J. Plasma Phys.* **75**, 731–748.

Stuart, B.C., Feit, M.D., Herman, S., Rubenchik, A.M., Shore, B.W. & Perry, M.D. (1996). Optical ablation by high-power short-pulse lasers. *J. Opt. Soc. Am. B* **13**, 459–468.

Svanberg, S. & Wahlstrom, C.G. (1995). *X-ray Lasers*. Bristol, UK: Institute of Physics, Bristol.

Tabak, M., Hammer, J., Glinsky, M.E., Kruer, W.L., Wilks, S.C., Woodworth, J., Campbell, E.M., Perry, M.D. & Mason, R.J. (1994). Ignition and high gain with ultrapowerful lasers. *Phys. Plasmas* **1**, 1626–1630.

Tajima, T. & Dawson, J.M. (1979). Laser Electron Accelerator. *Phys. Rev. Lett.* **43**, 267–270.

Treumann, R.A. (2001). Statistical mechanics of stable states far from equilibrium: thermodynamics of turbulent plasmas. *Astrophys. & Space Sci.* **277**, 81–95.

Treumann, R.A., Jaroschek, C.H. & Scholer, M. (2004). Stationary plasma states far from equilibrium. *Phys. Plasmas* **11**, 1317–1325.

Tsallis, C. (1988). Possible generalization of Boltzmann–Gibbs statistics. *J. Stat. Phys.* **52**, 479–487.

Vasyliunas, V.M. (1968). A survey of low energy electrons in the evening sector of the magnetosphere with OGO1 and OGO3. *J. Geophys.Res.* **73**, 2839–2884.